



Diagnosing the particle transport mechanism in the Geminga's pulsar halo via X-ray observation

Qi-Zuo WU

Nanjing University



Collaborator: Ruo-Yu Liu, Xuan-Han Liang, Jia-Shu Pan

TeVPA 2021
Chengdu, China



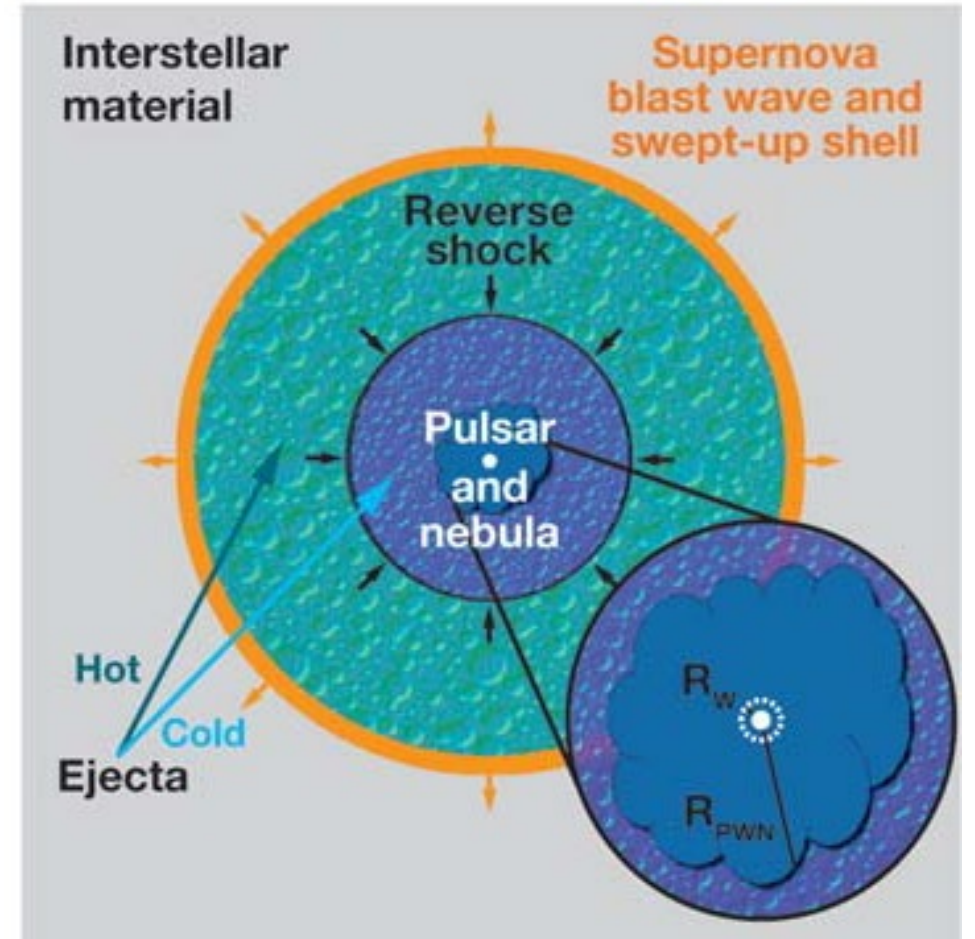
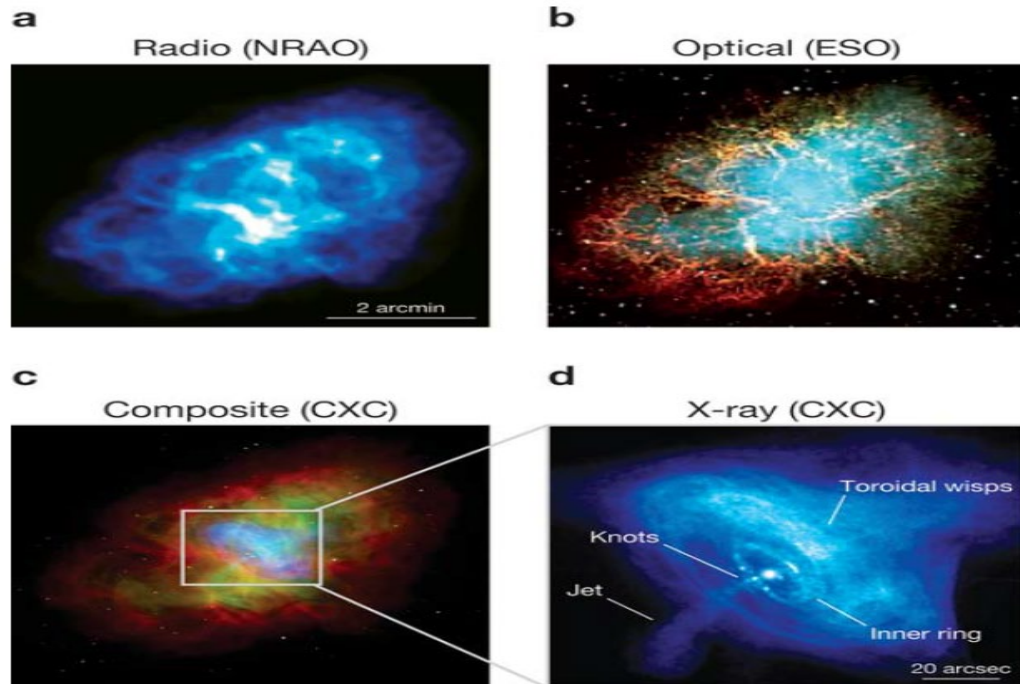


Pulsar and PWN

Pulsar : rapidly rotating , highly-magnetized neutron star

Rotational energy → electromagnetic energy

Pulsar wind nebula(PWN): a bubble of shocked relativistic particles



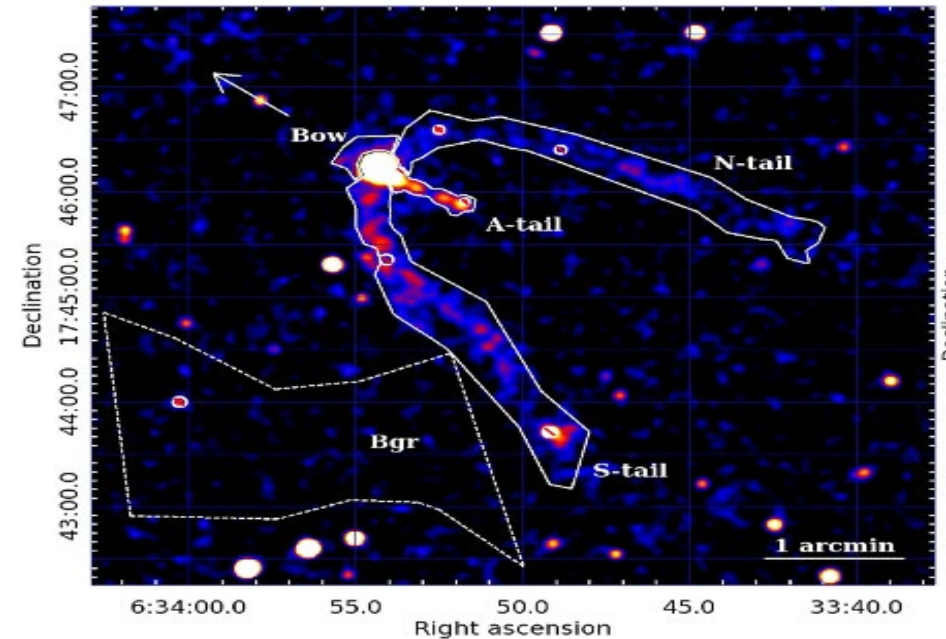
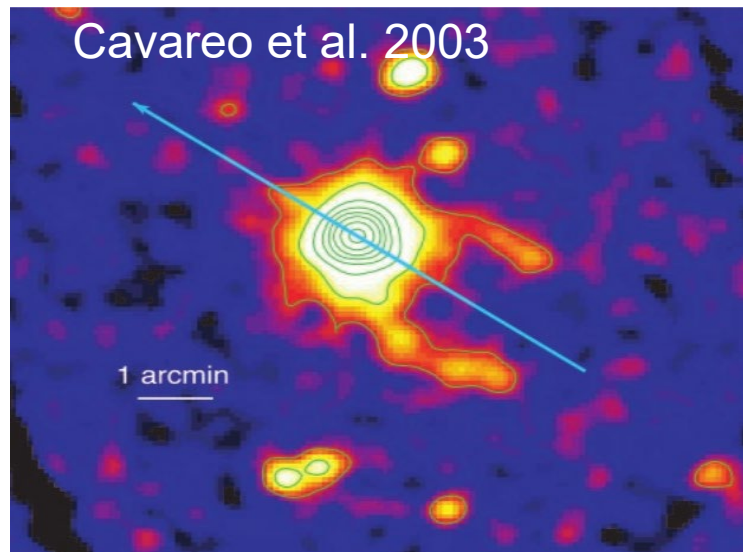
Geminga

One of the closest pulsar ($d=250\text{pc}$)

One of the brightest persistent GeV point source ($F_{>0.1\text{GeV}} \sim 10^{-10} \text{ergcm}^{-2}\text{s}^{-1}$)

characteristic age: 340 kyr

Geminga's PWN

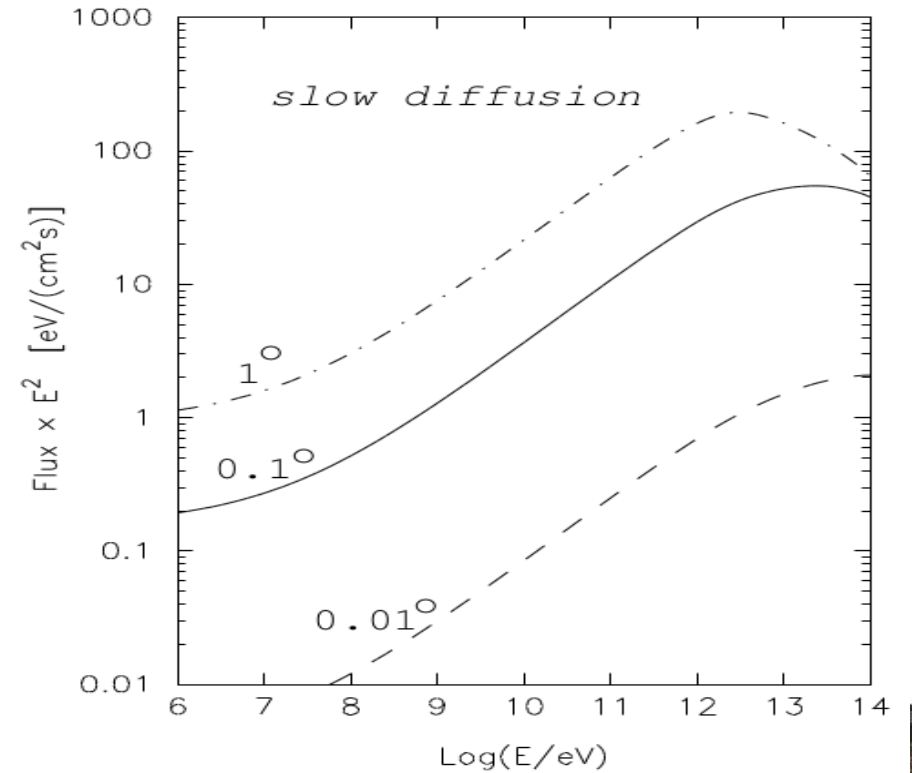
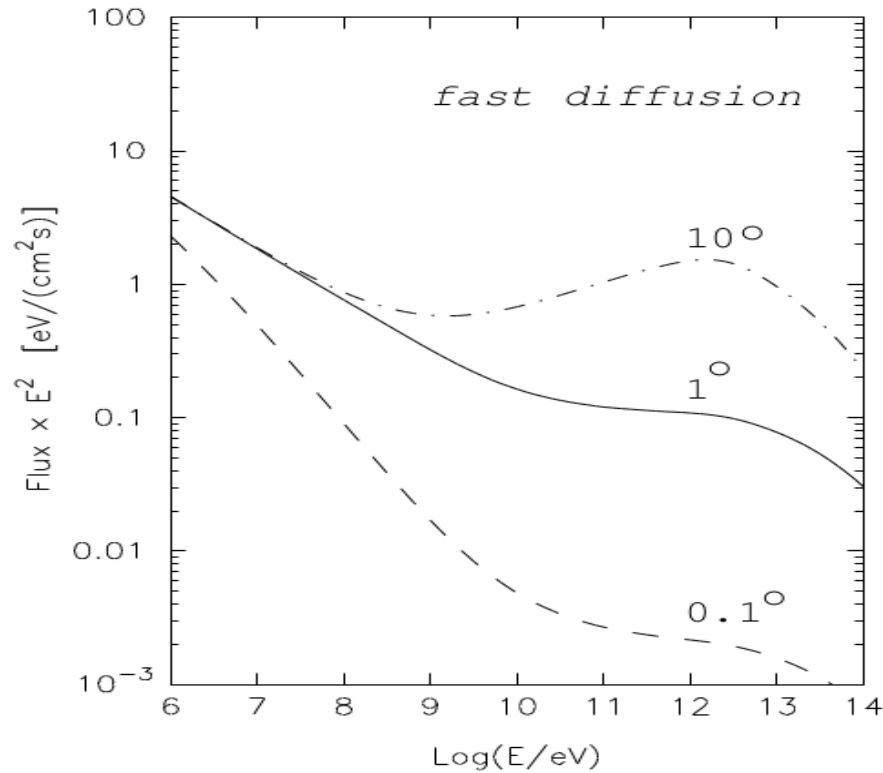




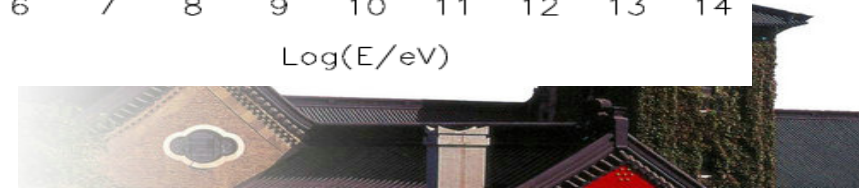
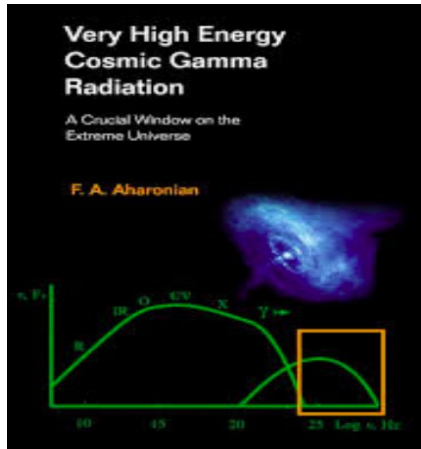
Prediction of halo around CR sources

Prediction of relativistic electron clouds expanding in the ISM around CRe sources

Inverse Compton of electrons on IR/CMB \rightarrow gamma ray

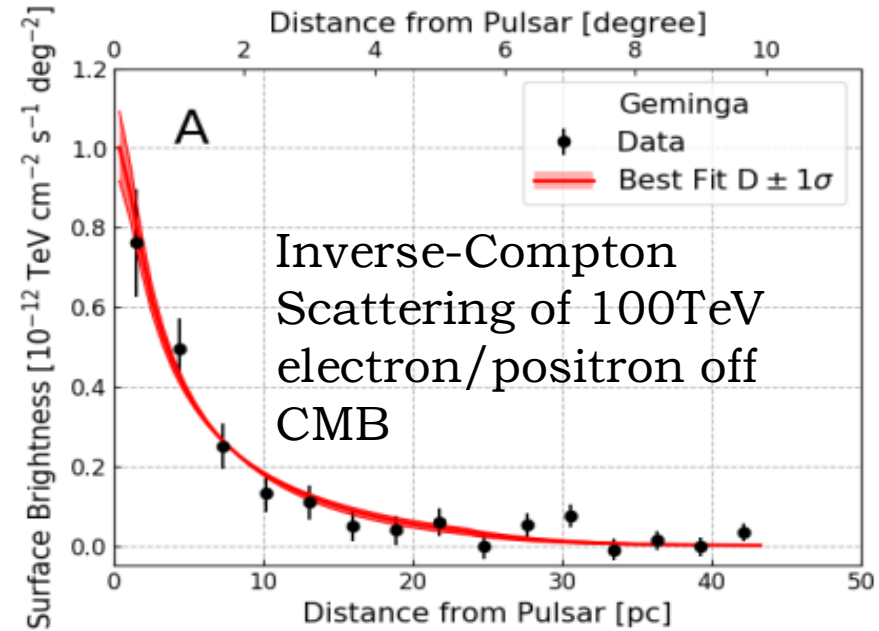
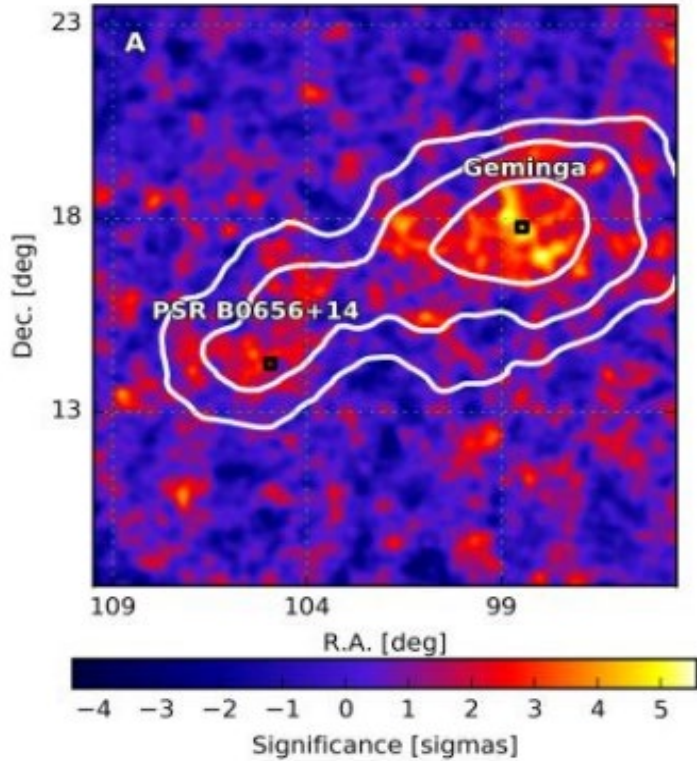


Aharonian 2004





HAWC's observation



HAWC Collaboration 2017,
Science, 2017, 358, 911

D_{100} (Diffusion coefficient of 100TeV electrons from joint fit of two PWNe)	$[x10^{27} \text{ cm}^2/\text{sec}]$	4.5 ± 1.2
--	--------------------------------------	---------------

Two orders of magnitude smaller than the typical ISM diffusion coefficient



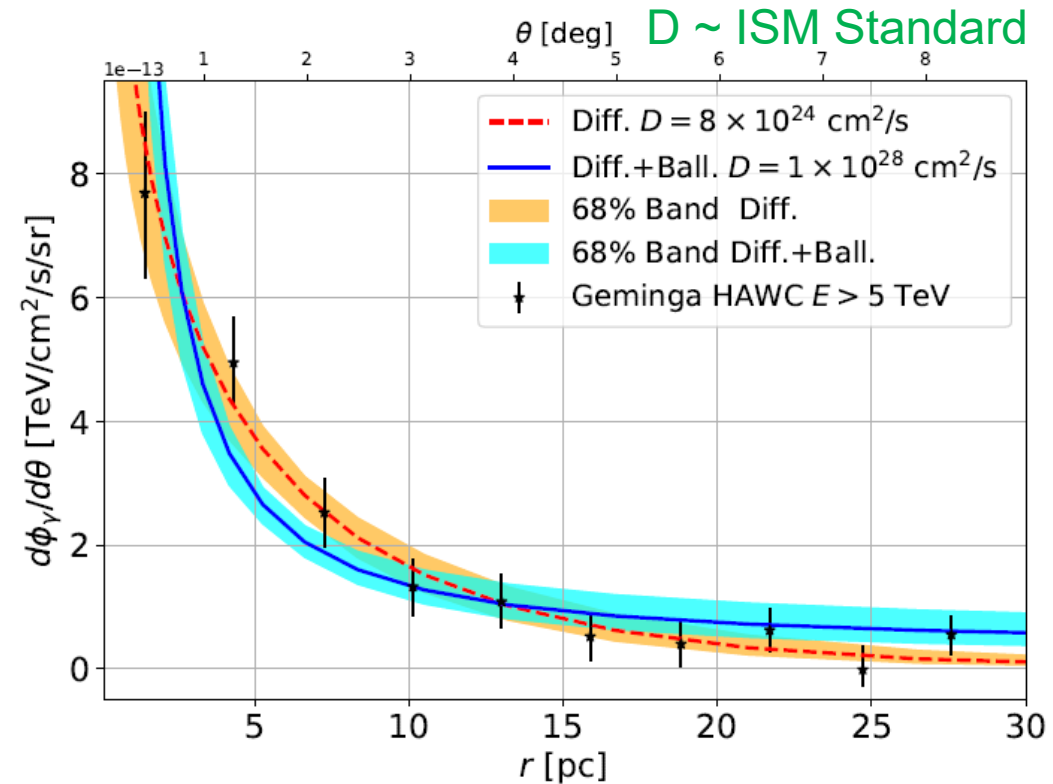
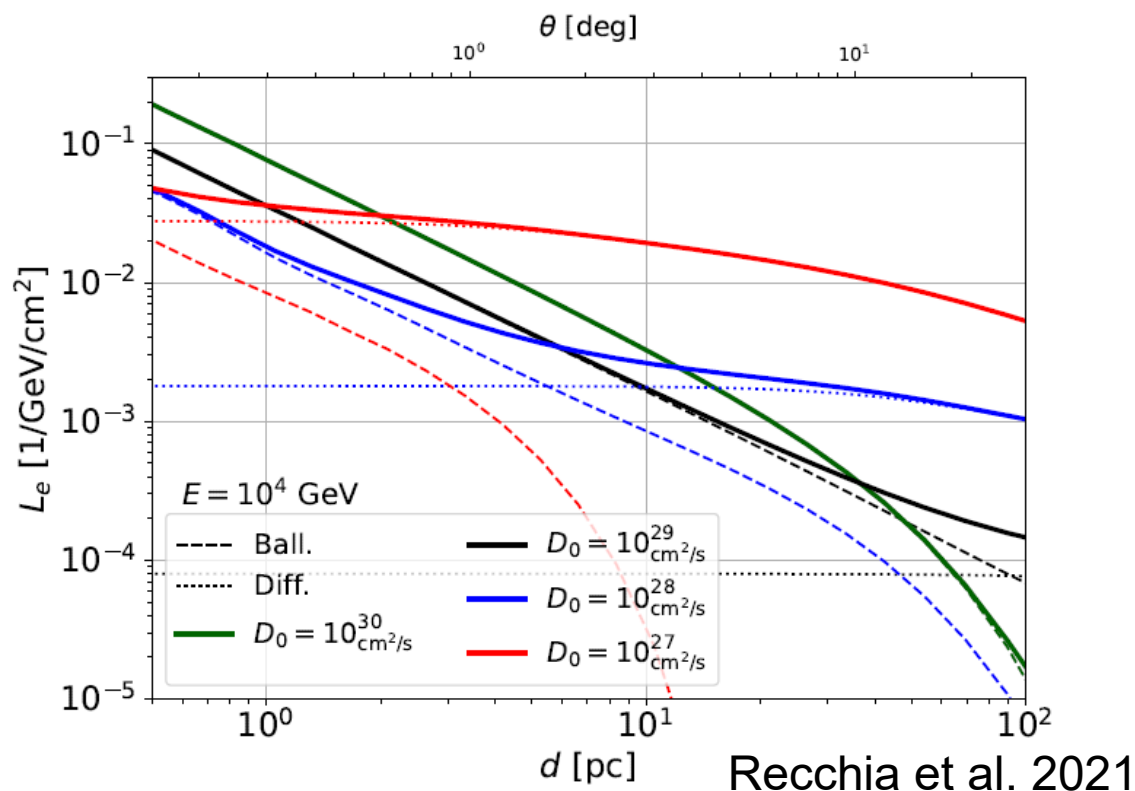


Diffusion model with Ballistic propagation

Quasi-ballistic → Diffusion

$$\tau_c = 3D(E)/c^2$$

$$f_{ball}(r, E) = \int_{T-\tau_c}^T \frac{Q(E)L(T)}{4\pi c^3 (T-t_0)^2} \delta\left((T-t_0) - \frac{r}{c}\right) dt_0 \quad f_{diff}(r, E) = \int_0^{T-\tau_c} dt_0 \frac{Q(E_0)L(t_0)}{\pi^{3/2} r_d^3(E, E_0)} \frac{b(E_0)}{b(E)} e^{-\frac{r^2}{r_d^2(E, E_0)}}$$





Anisotropic Diffusion

Z axis: Mean B field

$$M_A \sim \Delta B / B < 1$$

anisotropic

Diffusion coefficient -> Diffusion coefficient tensor

$$D_{zz} = D_{\parallel} = D_0 (E_e / 1\text{GeV})^q$$

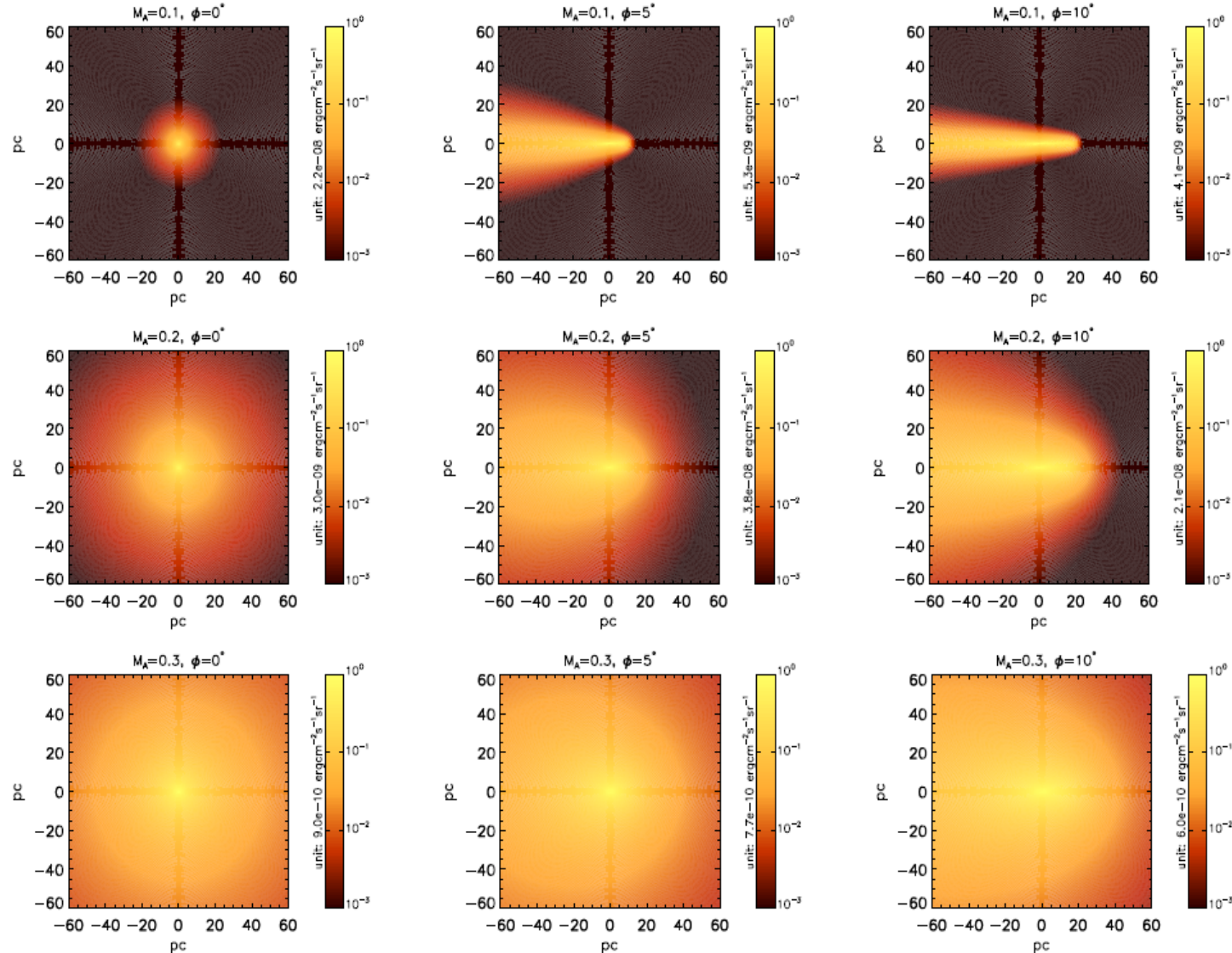
$$D_{rr} = D_{\perp} = D_{zz} M_A^4$$

Mean B field well aligned with LOS



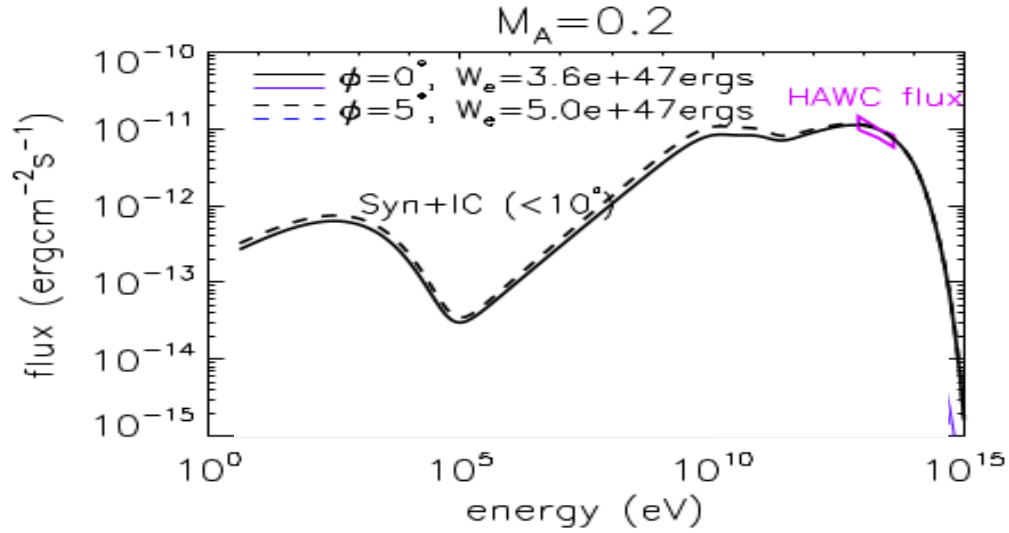
Horizontal: different viewing angle
Vertical: different Alfvénic Mach Number

Liu et al. 2019



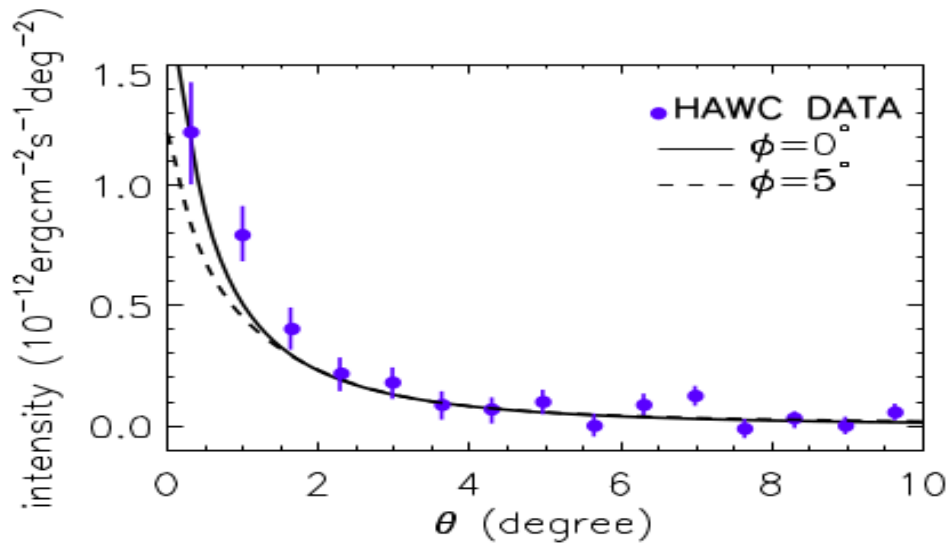


Anisotropic Diffusion



$M_A \sim 0.2, \phi < 5^\circ$

Mean B field well aligned with LOS

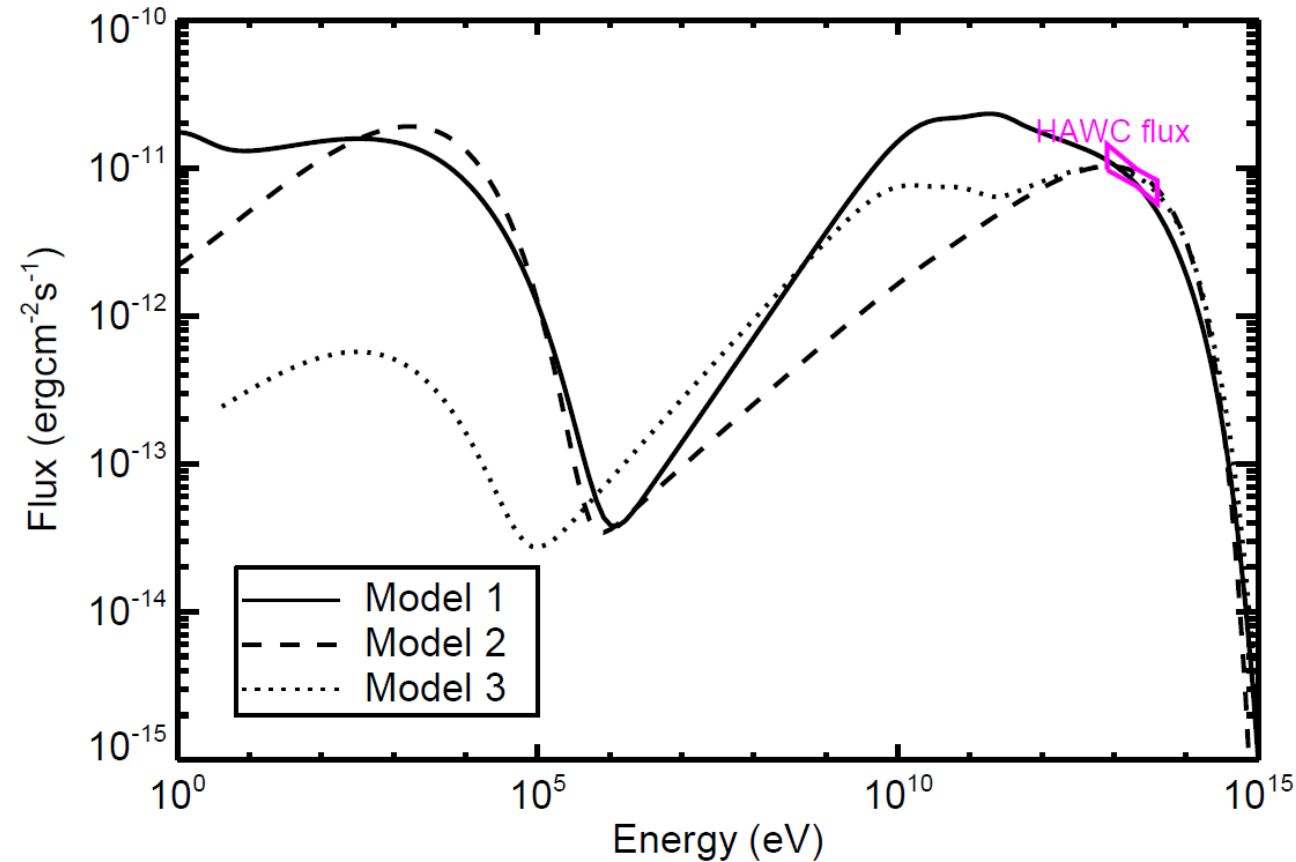
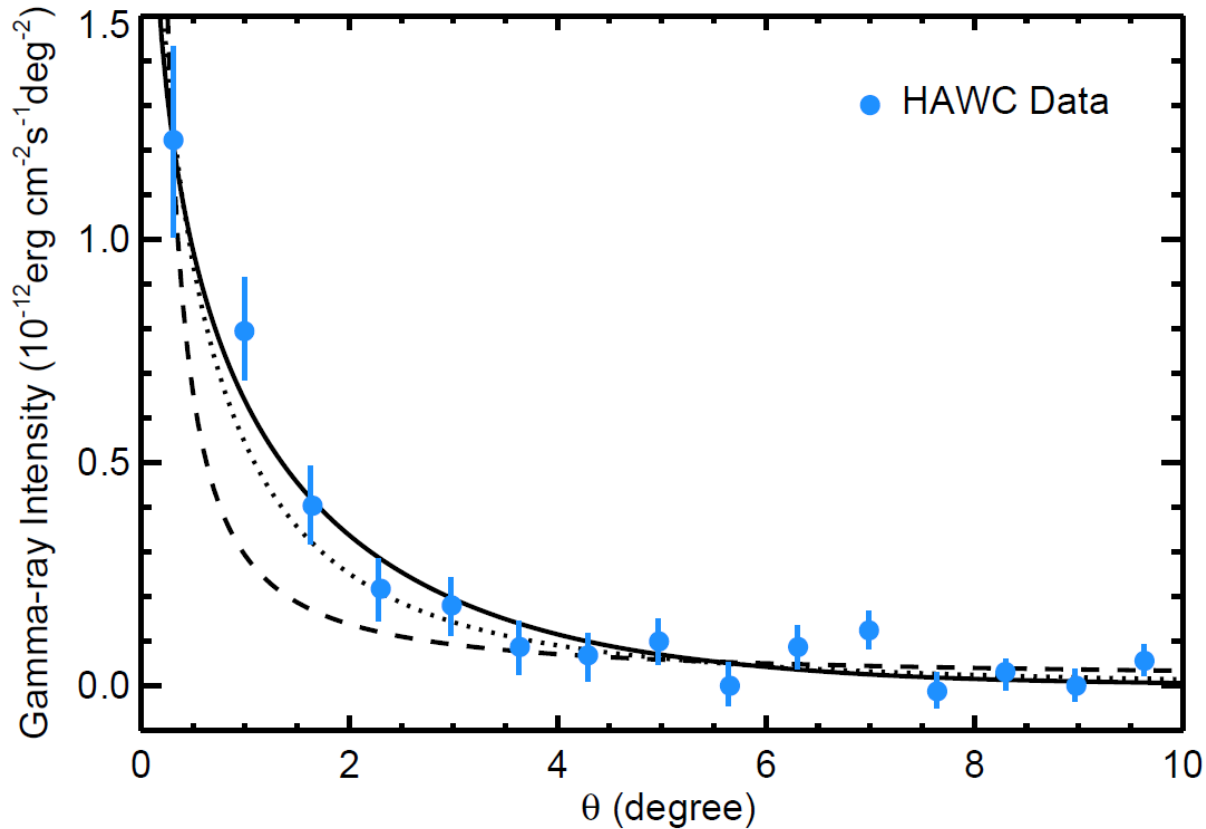




Fitting result

- Model 1: diffusion, isotropic
- Model 2: Ballistic + diffusion, isotropic
- Model 3: Diffusion, anisotropic

5-50 Tev Profile





Comparison between 3 models

	Transport mode	Diffusion coefficient	Magnetic topology	Field strength	e^\pm fraction η_e	Injection slope	Cutoff energy
Model 1	diffusion, isotropic	~1% ISM Standard	Highly chaotic	$3\mu\text{G}$	0.04	1.6	200TeV
Model 2	Ballistic + diffusion, isotropic	ISM Standard	Highly chaotic	$3\mu\text{G}$	1	1.6	100TeV
Model 3	Diffusion anisotropic	ISM Standard	with mean direction aligned with LOS	$3\mu\text{G}$	0.03	1.6	200TeV





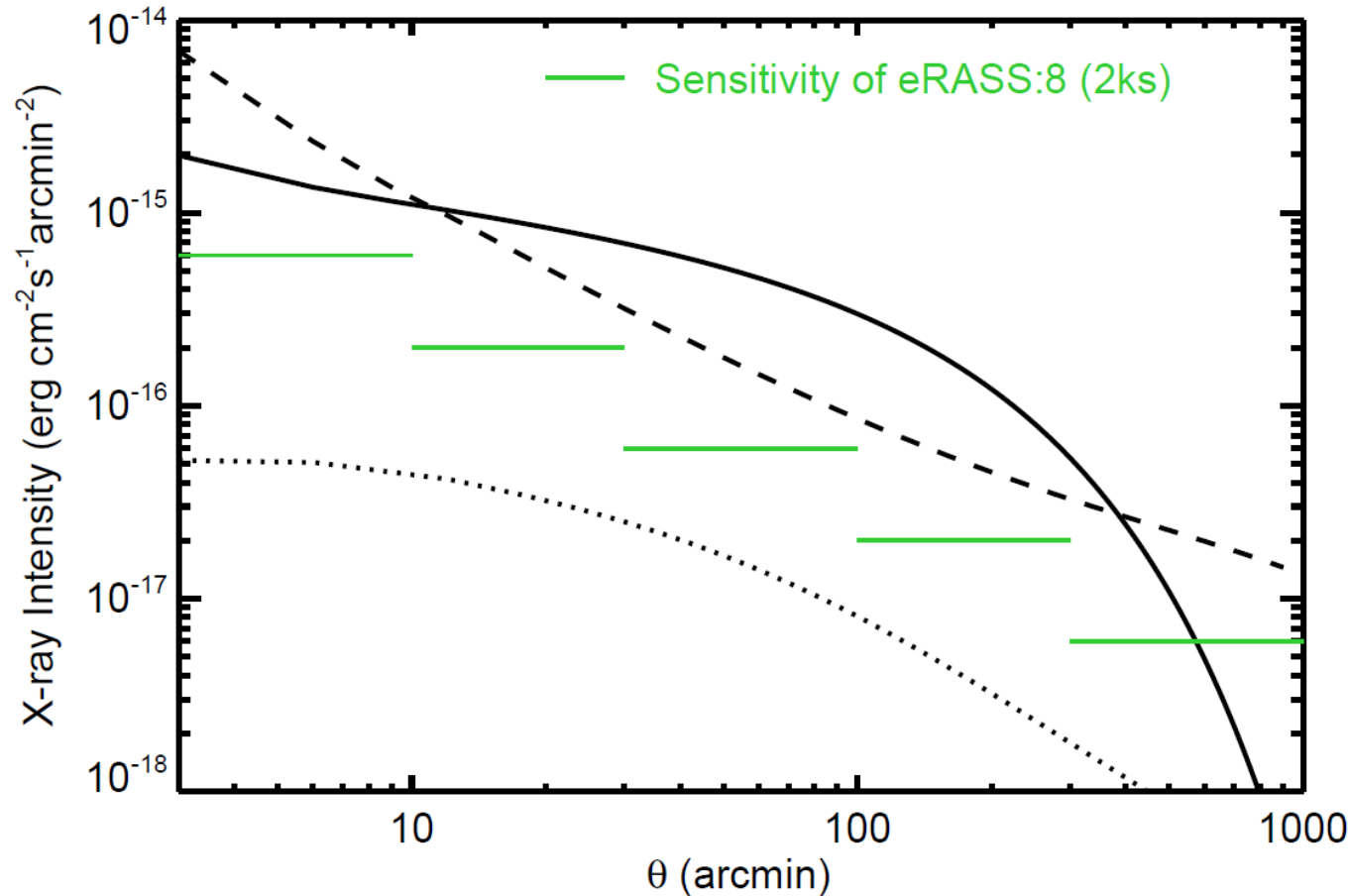
Surface Brightness Profile: 0.5-2 keV

- Model 1: diffusion, isotropic
- - - Model 2: Ballistic + diffusion, isotropic
- ⋯ Model 3: Diffusion, anisotropic

Model1 : Upper convex

Model2: Lower convex

Model 3: Low Intensity





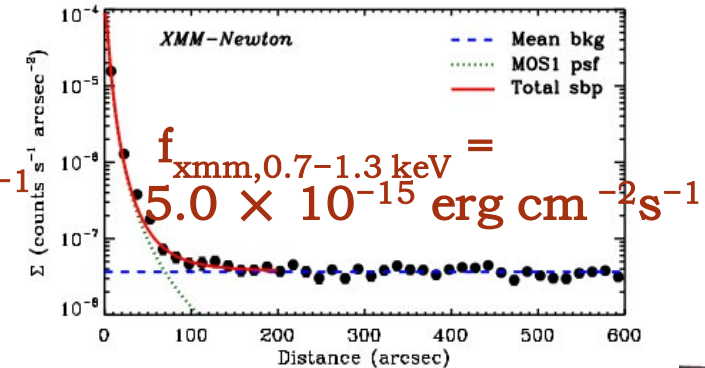
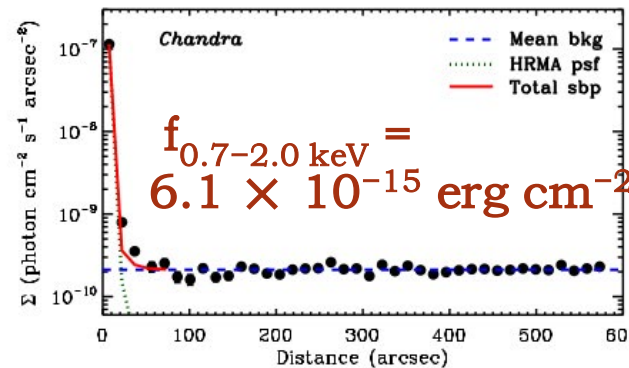
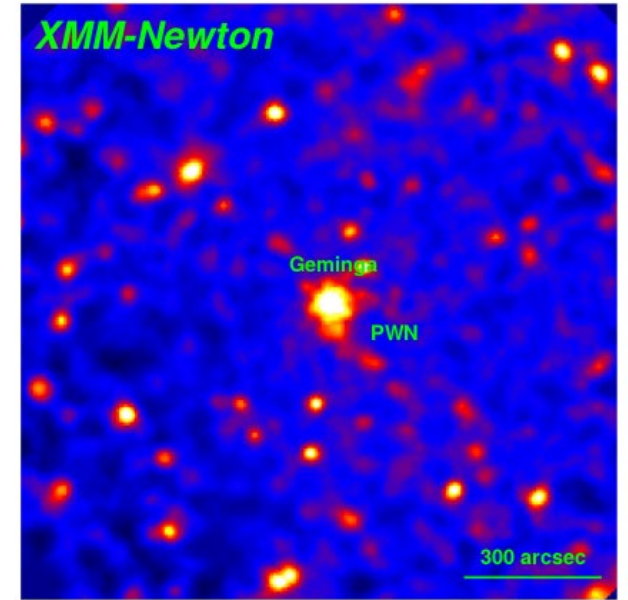
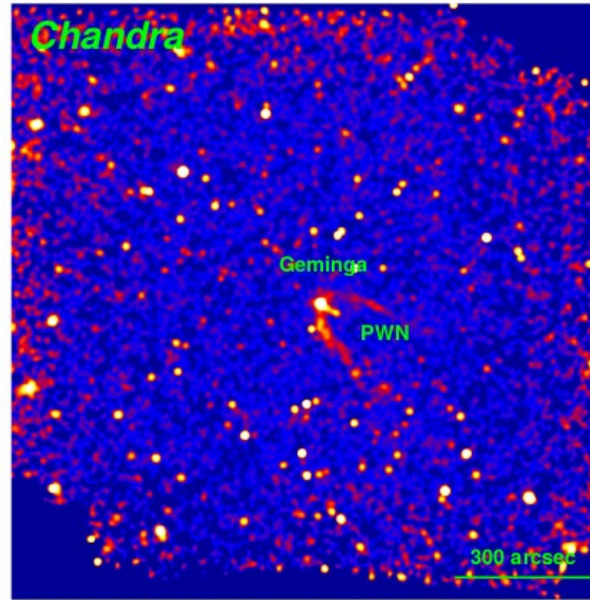
X-ray observation

Liu et al. 2019, ApJ

X-ray – Synchrotron radiation

Upper limit for X-ray flux in 600"

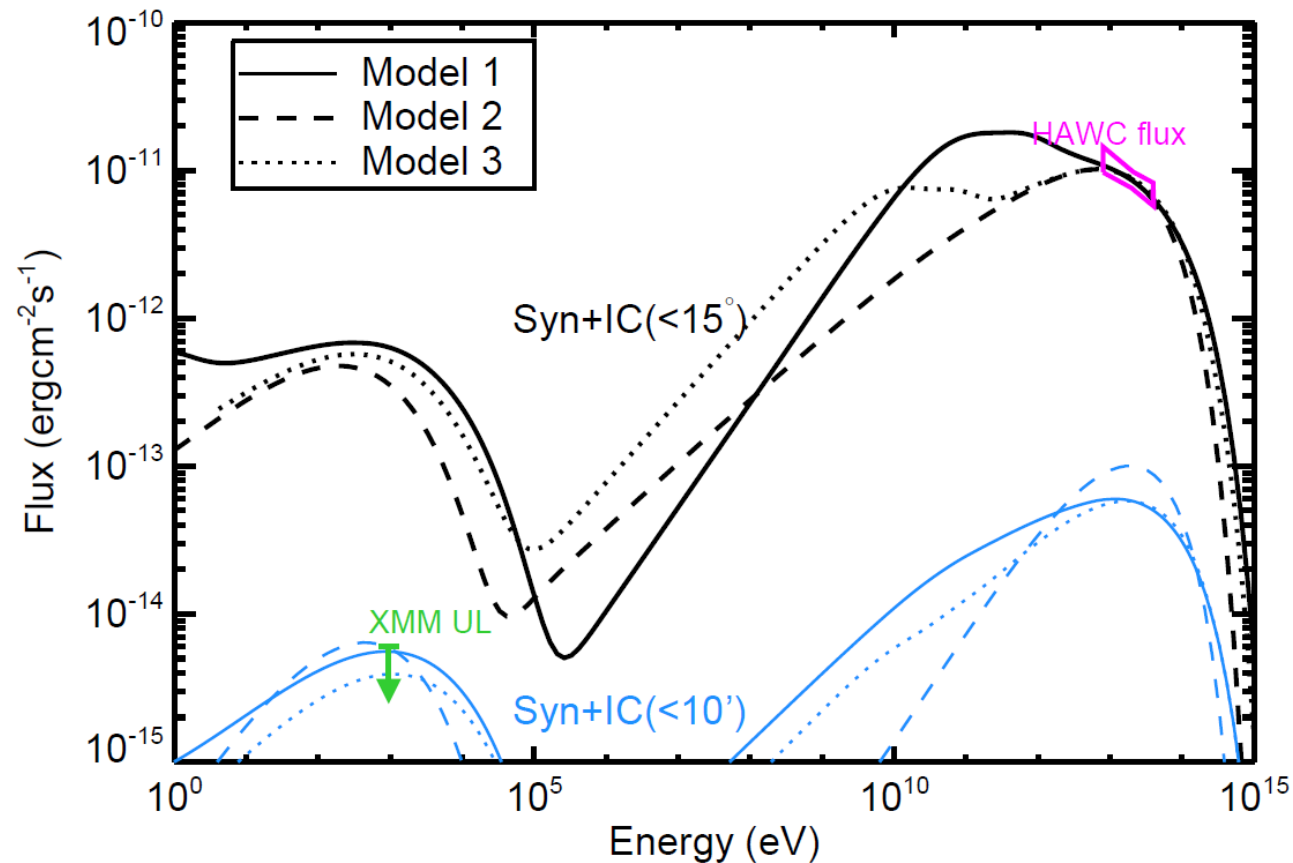
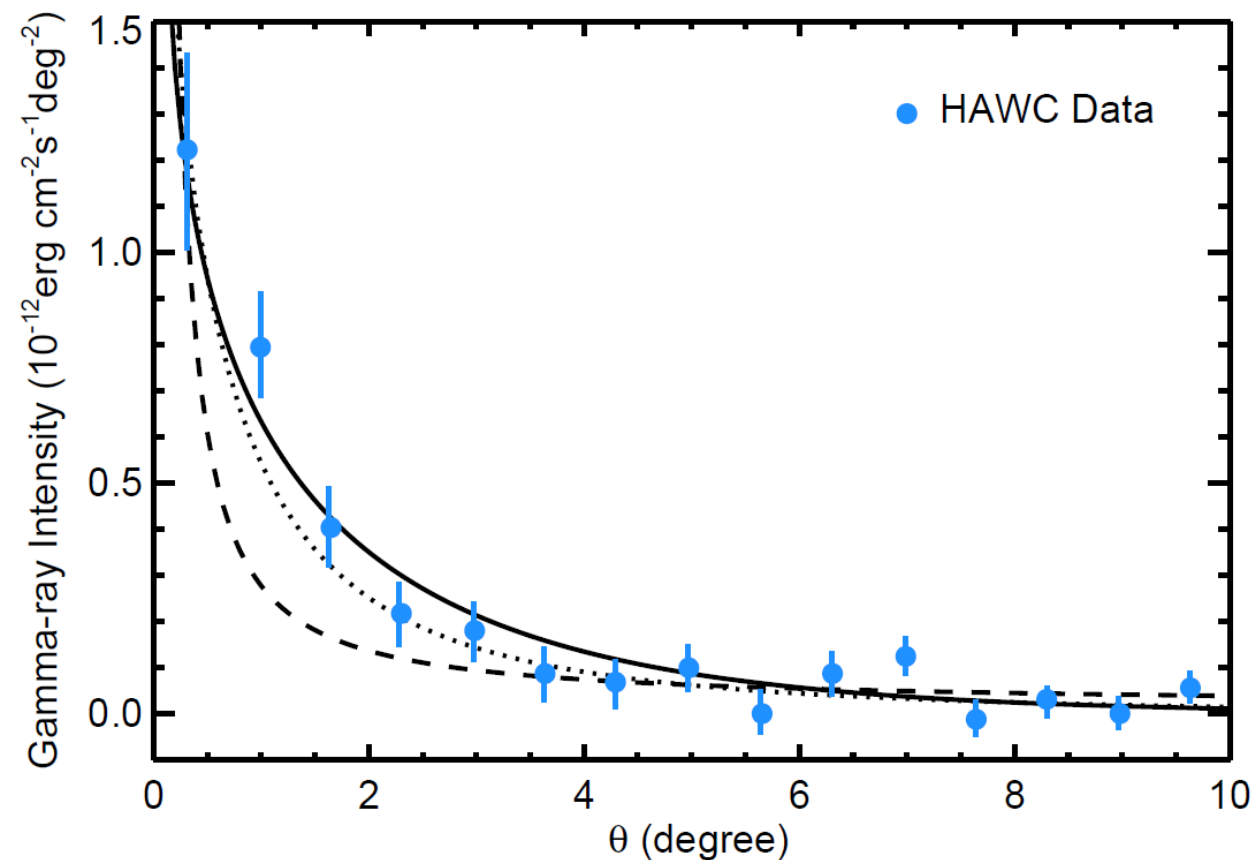
Central region: PSF
Outer region: Cosmic background





Fitting result (+X-ray UL)

- Model 1: diffusion, isotropic
- Model 2: Ballistic + diffusion, isotropic
- Model 3: Diffusion, anisotropic





Comparison between 3 models(+ X-ray UL)

	Transport mode	Diffusion coefficient	Magnetic topology	Field strength	e^\pm fraction η_e	Injection slope	Cutoff energy
Model 1	diffusion, isotropic	~1% ISM Standard	Highly chaotic	$0.6\mu\text{G}$	0.017	1.6	200TeV
Model 2	Ballistic + diffusion, isotropic	ISM Standard	Highly chaotic	$0.5\mu\text{G}$	1	1.6	80TeV
Model 3	Diffusion anisotropic	ISM Standard	with mean direction aligned with LOS	$3\mu\text{G}$	0.03	1.6	200TeV

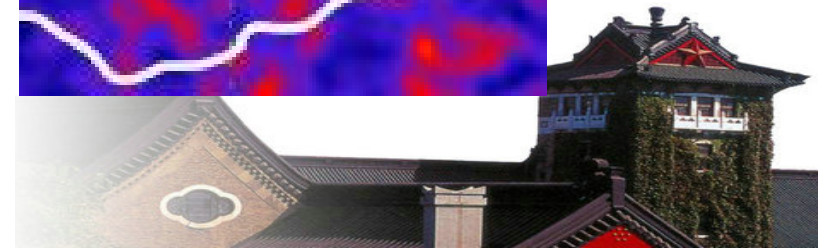
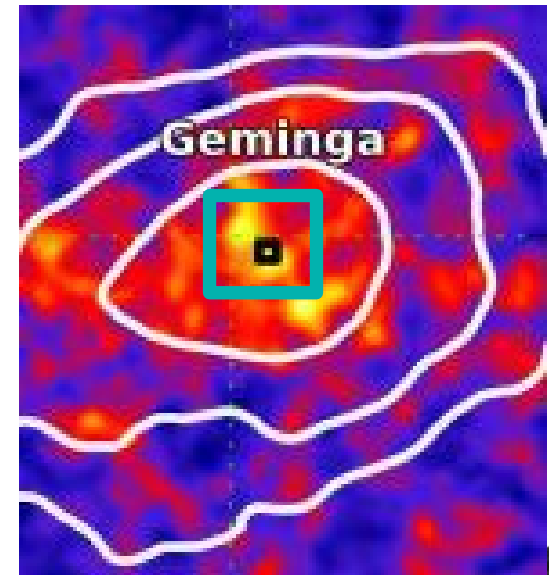
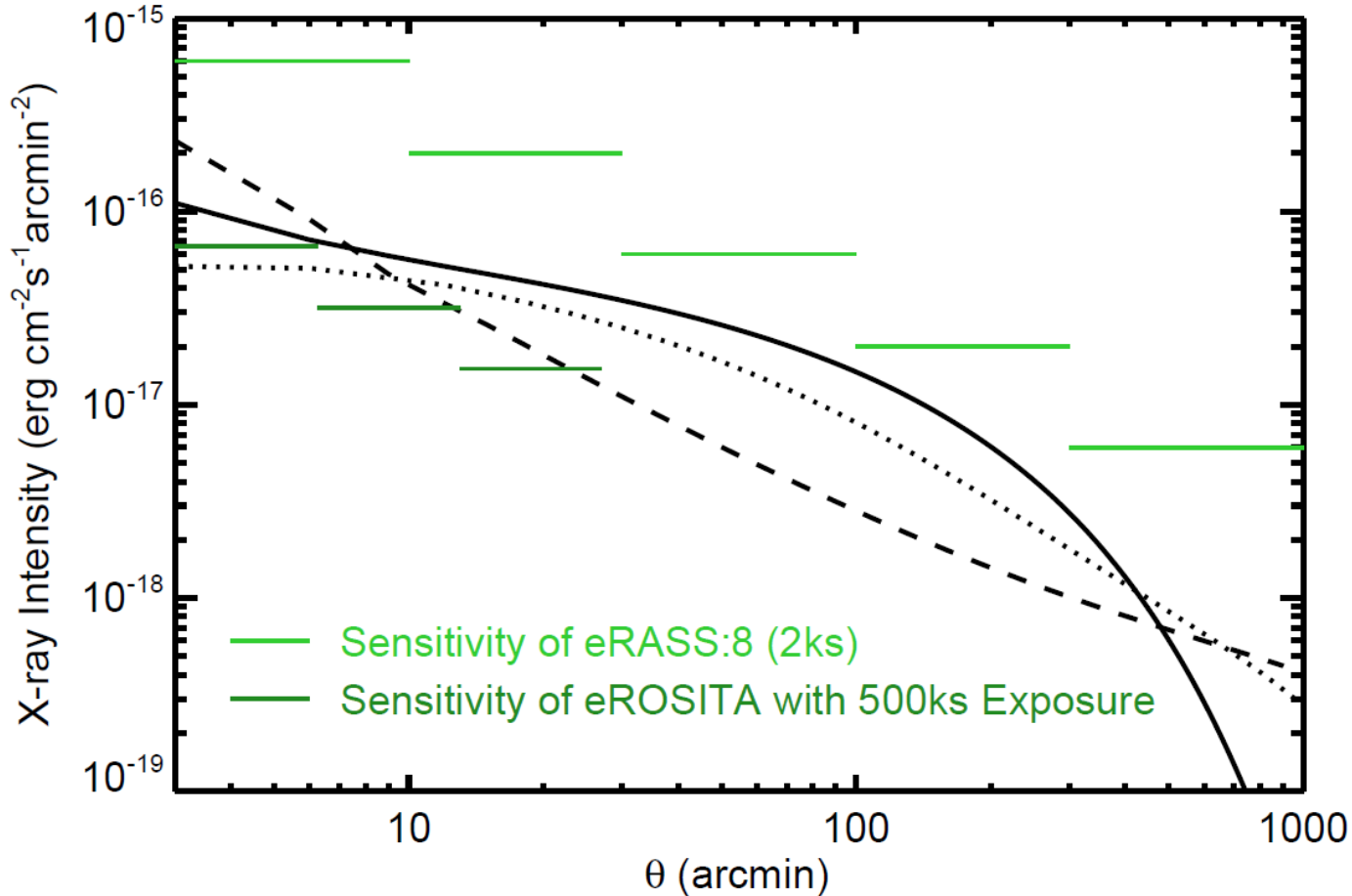




Surface Brightness Profile: 0.5-2 keV

Diagnosing the particle transport mechanism in the Geminga's pulsar halo via X-ray observation

+ X-ray UL





Summary

- HAWC data in gamma-ray can not distinguish three models for Geminga's Tev halo
- X-ray observation(eg.eRASS) can distinguish these models
- In fact,XMM-Newton and Chandra already shows no detection of the X-ray halo within central 10 ' region, implying a very weak $B(<1 \mu\text{G})$ for model 1 and model 2
- With a deep exposure(eg.500ks) on the central region of the halo,eRosita may still be capable of diagnosing the particle transport mechanism in the Geminga's pulsar halo

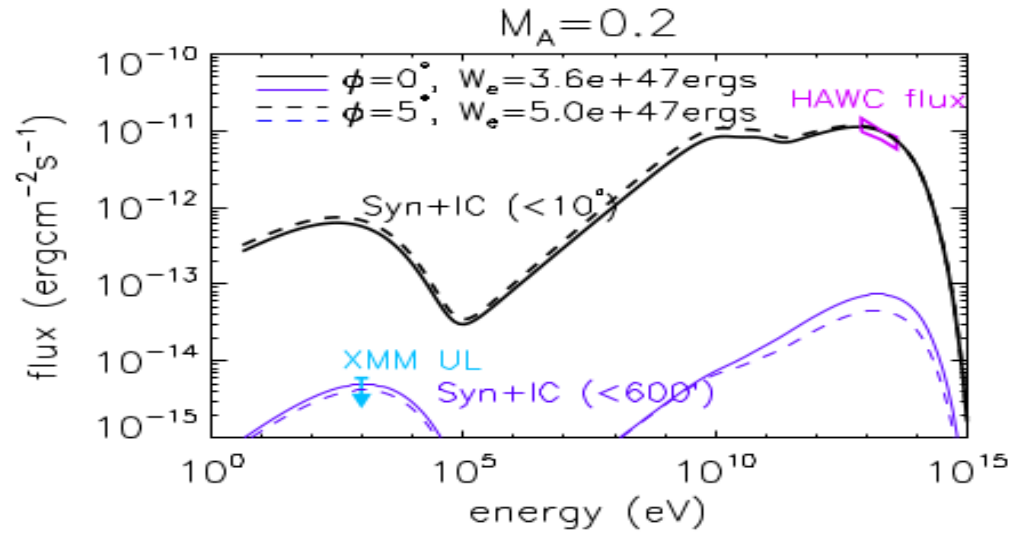


NANJING
UNIVERSITY



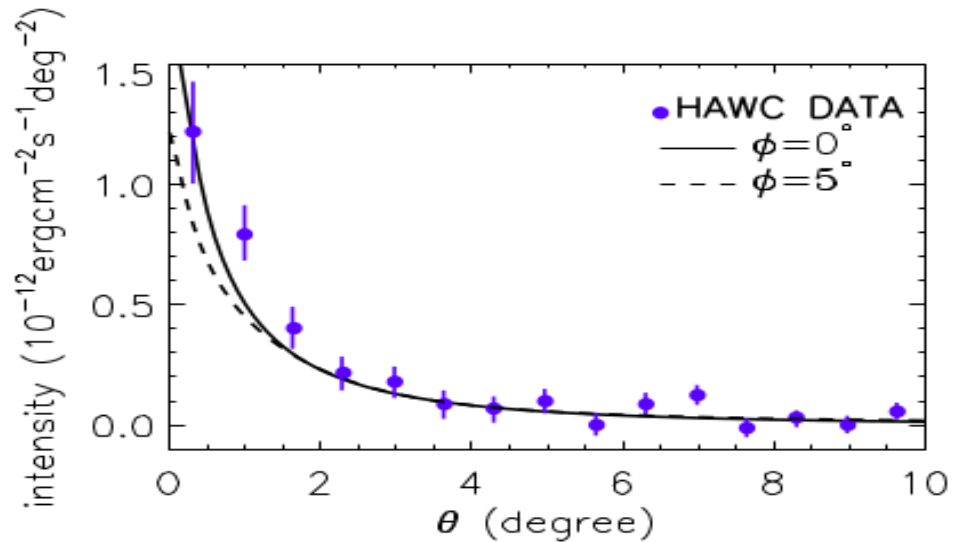
Question





$M_A \sim 0.2, \phi < 5^\circ$

Mean B field well aligned
with LOS



Mean B field in other TeV halos
cannot be always aligned with
LOS

